ENCLOSURE 4

APP-MP01-T2Y-002, Revision 1

"Environmentally Assisted Cracking Susceptibility Assessment of ***AP1000***®
RCP Flywheel Retainer Ring A 289 18Cr-18Mn Steel Material through Slow Strain
Rate Testing Under Simulated Primary Water Environment"

(Non-Proprietary)

Environmentally Assisted Cracking Susceptibility Assessment of *AP1000*[1]® RCP Flywheel Retainer Ring A 289 18Cr-18Mn Steel Material through Slow Strain Rate Testing Under Simulated Primary Water Environment

A White Paper

Gutti V. Rao

INTRODUCTION

This report summarizes the results of an autoclave Slow Strain Rate Test (SSRT) program undertaken by Westinghouse to establish the Environmentally Assisted Cracking (EAC) susceptibility of ***AP1000*** Reactor Coolant Pump (RCP) Flywheel Retainer Ring (A 289 18Cr-18Mn Steel) material under simulated RCS environment representing "beyond design basis" condition of leakage in the Alloy 625 hermetically sealed flywheel can. The testing is performed at the request of the Advisory Committee on Reactor Safeguards (ACRS) in order to establish the adequacy of retainer ring material Stress Corrosion Cracking (SCC) performance under continued operation beyond the design basis condition, representing the unlikely event of breaching in the Alloy 625 flywheel can of the RCP which would result in the exposure of the retainer ring to primary water.

The ***AP1000*** reactor coolant pump design consists of ASTM A289 18Cr-18Mn alloy steel material for the flywheel retainer ring which holds the high density [ ]^{a,c} inserts. **Figures 1 and 2** illustrate the sectional drawings of the Pump and the Flywheel configurations respectively, showing the locations of the [ ]^{a,c} inserts, inner hub and the retainer ring, enclosed in the hermetically sealed Alloy 625 can. As part of the manufacturing process, the flywheel assembly is subjected to detailed inspections at various stages of assembling and the entire flywheel assembly is then hermetically sealed within a welded alloy 625 can which is inspected using a helium leak detection system. Under normal operating conditions in service, the retainer ring is completely separated from exposure to any primary water. Years of successful manufacturing experience with this alloy for electric generator use in the non-nuclear industry have not resulted in any issues. However, ACRS expressed desire to demonstrate safe continued operation without any SCC issues as a result of the postulated unlikely event of breaching of the Alloy 625 can weld. The ACRS was also interested in additional data because there is very little service experience or test data available in the literature on the performance of A289 material under exposure to primary water environment. The current program is undertaken to support the ACRS request.

[1] *AP1000 is a trademark* or registered trademark of Westinghouse Electric Company LLC, its affiliates and/or its subsidiaries in the United States of America and may be registered in other countries throughout the world.

PERFORMANCE HISTORY OF A289 18CR-18MN ALLOY STEEL

The 18Mn-18Cr (18/18) flywheel retainer ring material has been developed as a replacement material to the previous and more widely used 18Mn-4.5Cr (18/4) in generator rotor retainer rings. The 18/4 retainer rings were installed for decades until the mid 1970s but have been the subject of several failures in service. The 18/18 material was developed (Ref. 1, 2) for better stress corrosion resistance, higher strength and fracture toughness properties, and has been in use since 1978. Typical material property data reported in the literature for the 18/18 material which is stretched (cold worked) to a yield strength level of 195 ksi at mid-wall level, includes 18% elongation and 60% reduction in area with an impact energy of 126 ft-lbs. The higher fracture toughness of 18/18 renders the material relatively insensitive to minor defects.

Prior to its deployment in electric generation industry, 18Cr-18Mn was evaluated to verify superior corrosion resistance compared to the 18Mn-4Cr alloy (Refs. 1 and 2). Stress corrosion tests were conducted using smooth specimens in ambient temperature de ionized water, 1% ammonium nitrate solution, and 1% sodium chloride solution. Specimens survived yield strength level stresses for up to 50,000 hours without any failures. Pre-cracked three-point bend specimens were also tested at 175°F at a stress intensity factor of approximately 78 ksi $\sqrt{in}$ in the same environments for 2000 hours without any failures. The ammonium nitrate and sodium chloride environments are considered more aggressive than primary water. The 18Cr-18Mn retainer rings have been used since late 1970s without any reported stress corrosion failures (Refs. 2, 3, and 4).

SLOW STRAIN RATE (SSR) TESTING AND EAC SUSCEPTIBILITY

Slow Strain Rate (SSR) testing is an accelerated test method by which axially-loaded, tensile test specimens are slowly strained (usually in the range of 10^{-4} to 10^{-7}/s) to failure in a test environment in order to evaluate metallic material susceptibility to environmentally-assisted cracking (EAC). Environmentally-assisted cracking is cracking of a material caused by the combined effects of stress and the surrounding environment, and includes as examples: stress corrosion cracking, hydrogen embrittlement cracking, sulfide stress cracking, and liquid metal embrittlement. ASTM Method G129 (Ref. 6) provides standard guidelines, requirements, and recommendations for performing SSR testing and is the basis for the testing approach described in this test plan. SSR testing is typically performed in both the environment of interest (i.e., chemistry and temperature) and in an inert control environment (typically air or nitrogen) that has been shown not to cause EAC in the material under evaluation. The resulting stress profiles, the geometry changes in the samples, and the fracture surfaces are then compared to determine if the test environment influenced the cracking of the sample. A significant environmental effect indicates that there is the potential for the material to experience EAC when exposed to operation under the tested conditions.

SCOPE OF THE TEST PROGRAM

The current report is concerned with slow strain rate testing of ASTM A289 alloy steel retaining ring material in simulated Pressurized Water Reactor (PWR) primary system coolant. The testing was performed [ ]^{a,c} per Westinghouse Electric Company (WEC) requirements outlined in Westinghouse Purchase Order [ ]^{a,c}. The results of the testing are detailed in Reference 7.

The testing was undertaken in two phases:

- **Preliminary Screening testing** was performed at a strain rate of [ ]^{a,c} under Phase 1 tests. One environmental test with prototypical primary coolant and one replicate control test in [ ]^{a,c} were performed and the results of the two tests compared in order to assess susceptibility to EAC. Due to a test deviation that occurred during the preliminary environmental test (Test 1A-A), the environmental test was subsequently repeated (Test 1A-B)). The results from both tests have been included in this report.

- **Slower Strain Rate Susceptibility testing** was performed at a strain rate of [ ]^{a,c} under Phase 2. Two environmental tests with prototypical primary coolant and one control test in [ ]^{a,c} were performed and the results of the two test types compared in order to assess susceptibility to EAC. Tests at lower strain rates are more sensitive to the occurrence of EAC.

The primary coolant environment was maintained close to [ ]^{a,c}, which represents a [ ]^{a,c}. The concentration of hydrogen was maintained at [ ]^{a,c}. The test temperature was maintained at [ ]^{a,c}.

TEST MATRIX AND TEST SPECIMENS

A summary of the two phase SSR test matrix is provided in Table-1. The preliminary (Phase 1) tests consisted of higher strain rate ([ ]^{a,c}) screening tests while the second phase tests conducted at a slower strain rate ([ ]^{a,c}) will enhance the material exposure for EAC susceptibility assessment. In each phase duplicate tests were carried out in the primary water environment while only one test was conducted in the inert dry environment reference testing. The primary water chemistry environment and the test temperatures employed for each of the tests are also specified in the test matrix. All testing was performed in accordance with guidelines specified in ASTM G129 (Ref. 6).

The test specimens were fabricated from A289 Class 8 material, with Heat no. [ ]^{a,c} supplied from the pump vendor EMD. The specimens were machined at Westinghouse facilities located in New Stanton PA. The specimens were machined as smooth round tensile test specimens per ASTM E8 (Ref. 8) and had a diameter of [ ]^{a,c} in the test region with an effective gauge length of [ ]^{a,c}. All specimens were cut from a single retaining ring section as shown in **Figure 3**. Sets of specimens from the same radial location (i.e., all from the region of the ring closer to the inner diameter or all from the region of the ring closer to the outer diameter) were used in each test case series in order to minimize potential variances in pre-existing material conditions. Specifically, [ ]^{a,c} The geometry and dimensions of the test specimen are typically illustrated in **Figure 4**.

TEST PROCEDURES

- Tensile test control and monitoring (load and displacement) were performed using an [ ]^{a,c} servo ball-screw actuator (see **Figure 5**). This servo assembly contained instrumentation for displacement / load monitoring and control. A custom shaft assembly attached to the load cell of the servo assembly penetrated the upper head of [ ]^{a,c} autoclave vessel [ ]^{a,c}. A custom load frame was installed in the autoclave vessel containing appropriate grips designed per the requirements of ASTM E8 (Ref. 8) for attaching to the test specimen. [ ]^{a,c} All tests were performed to failure of the test specimens.

- The chemistry for the primary coolant environment was [ ]^{a,c}. Autoclave effluent samples were acquired at the start and end of each test. These samples were analyzed for F^-, Cl^-, SO_4^{-2}, and Zn. All samples were found to meet the EPRI primary water chemistry guidelines for anions (i.e., <150 ppb F^-, Cl^-, SO_4^{-2}) and to contain less than 20 ppb Zn.

- The concentration of hydrogen in the primary coolant was maintained at [ ]^{a,c} by maintaining hydrogen overpressure of [ ]^{a,c} and a temperature of [ ]^{a,c} in a bubble column reservoir (tall column with hydrogen sparging) feeding the autoclave. The hydrogen overpressure was continuously logged using a separate pressure transducer. Dissolved oxygen in the bubble column was monitored and logged at all times to ensure that equilibrium has been attained and that oxygen was less than [ ]^{a,c}. The data acquisition software contained user-configurable high and low alarms for hydrogen bubble column overpressure and a high alarm for dissolved oxygen. Direct measurements of dissolved hydrogen concentration were not made.

- The target test temperature in the autoclave for both environmental and control tests was [ ]^{a,c}. For both environmental and control tests, the temperature was controlled/measured using a thermocouple that was press-fit into a hole in the lower grip section of the test specimen.

- For the slower strain rate environmental susceptibility tests, the autoclave was maintained at a pressure of [ ]^{a,c}, which was sufficient to prevent boiling and to maintain hydrogen solubility (i.e., greater than the sum of the vapor pressure for [ ]^{a,c} water [ ]^{a,c} plus the equilibrium partial pressure for hydrogen at the maximum dissolved hydrogen limit of [ ]^{a,c} and target water temperature of [ ]^{a,c}. Pressure control was achieved by maintaining a solid water (i.e., hydraulic) system in the autoclave using a positive displacement injection pump with a backpressure regulator set at the target pressure on the autoclave effluent. For the control tests, the autoclave was maintained at the same pressure with [ ]^{a,c} being slowly bled through the vessel.

- For the slower strain rate environmental susceptibility tests, the autoclave was refreshed at a rate of [ ]^{a,c}. Based on the [ ]^{a,c} autoclave volume and [ ]^{a,c} volume displaced by the specimen load frame, this corresponds to a turnover time of [ ]^{a,c}. For the control tests, [ ]^{a,c} gas was bled through the autoclave at a rate of [ ]^{a,c}. The [ ]^{a,c} bleed rate was selected to ensure that a [ ]^{a,c} was sufficient for the longer [ ]^{a,c} sensitivity tests and to ensure that the flow was measurable with the same autoclave effluent flowmeter that was used for the environmental tests [ ]^{a,c}.

- [ ]^{a,c} gas was bled through the autoclave at a rate of [ ]^{a,c}. The [ ]^{a,c} bleed rate was selected to ensure that a [ ]^{a,c} was sufficient for the longer [ ]^{a,c} sensitivity tests and to ensure that the flow was measurable with the same autoclave effluent flowmeter that was used for the environmental tests [ ]^{a,c}.

flywheel configurations

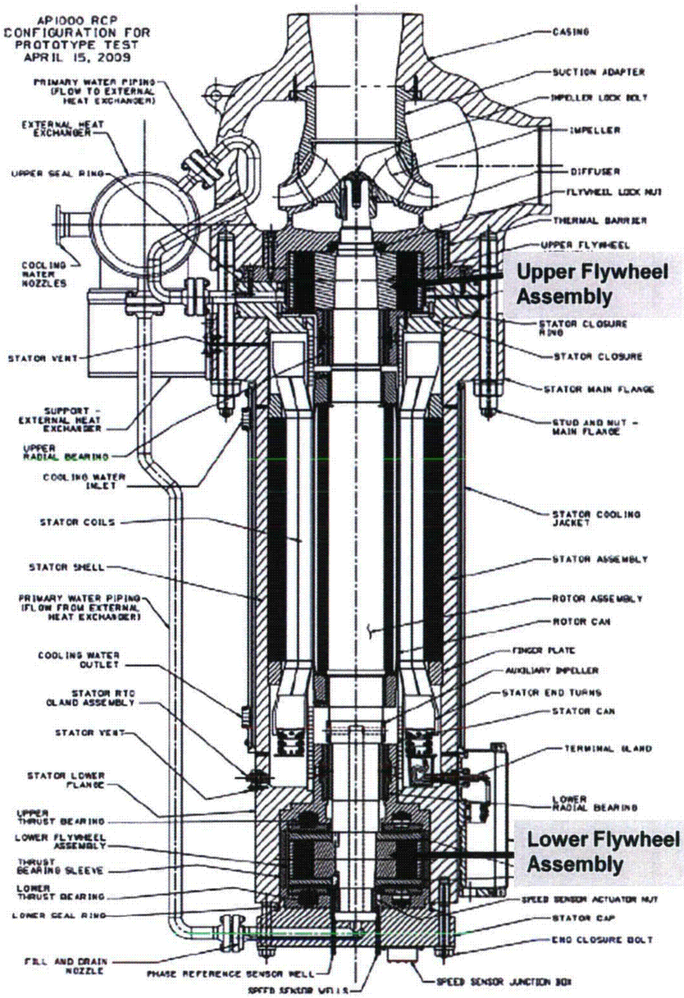

Figure 1. Sectional View of AP1000 RCP Showing the Upper and Lower Flywheel Assembly Regions

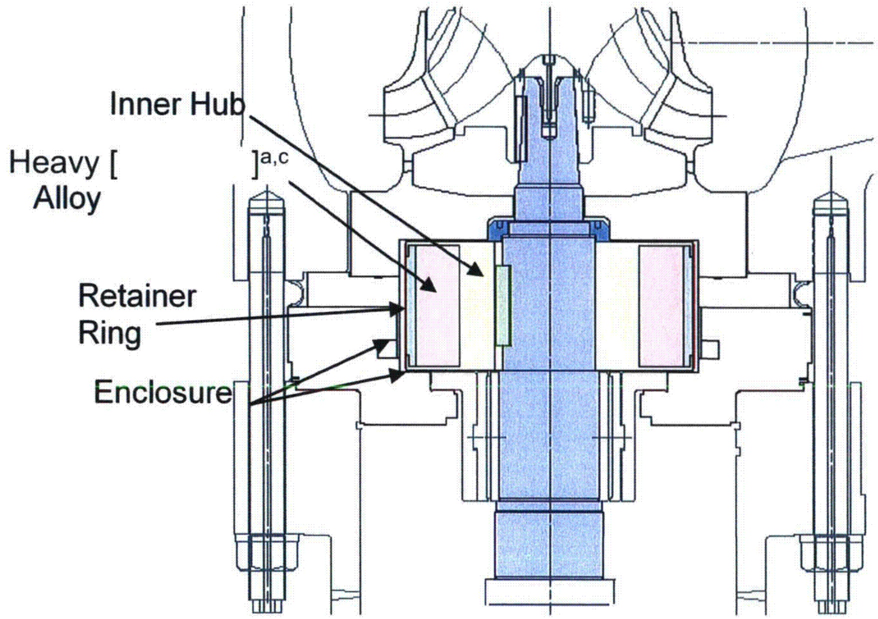

Figure 2. Details of the Flywheel Assembly Region

TEST RESULTS AND DISCUSSION

Stress-Strain Curves and Deformation Behavior

A comparison of the resulting stress-strain curves for each of the six SSR tests is illustrated in **Figure 6**. **Figure 7** shows a similar comparison but only for the three preliminary phase 1 tests while **Figure 8** shows the same comparison for just the three slower strain rate susceptibility sensitivity tests under Phase 2. Specimens cut from the outer diameter of the retaining ring section and exposed to the higher [ ]a,c strain rate (i.e., preliminary test specimens) exhibited a [ ]a,c yield stress of approximately [ ]a,c, and specimens cut from the inner diameter of the retaining ring section and exposed to the slower [ ]a,c strain rate (i.e., phase 2 test specimens) exhibited a [ ]a,c yield stress of approximately [ ]a,c (see Table 2). These results are consistent with the base line tensile test results obtained at the Westinghouse test facilities which can be used to estimate a [ ]a,c yield strength of [ ]a,c at the target test temperature of [ ]a,c. All stress-strain curves demonstrated evidence of ductile specimen necking as the engineering stress gradually decreased after yield before more rapidly decreasing necking prior to fracture. Necking and ductile fracture were confirmed with post-test examination of the fractured specimens, with fracture occurring within the middle 50% of the gauge length for all specimens. The classical cup and cone ductile fracture exhibited by one of the phase 2 environmental susceptibility test specimen is illustrated in **Figure 9**.

Per the guidelines described in ASTM G129, susceptibility to EAC can be assessed using stress-strain test data (time-to-failure ratio, plastic elongation ratio, ultimate tensile strength, and fracture energy), specimen measurements (elongation and area reduction), and microstructural analyses (optical microscopy of fracture, Scanning Electron Microscopy (SEM) evaluation of fracture surface morphology). Stress-strain results and specimen measurements are evaluated quantitatively by calculating a ratio for each parameter that compares the value obtained in the environment of interest to that obtained in the inert control environment. Lower values for these SSR ratios generally indicate increasing susceptibility to EAC. However, there have been reported cases where decreasing SSR ratios have been observed in smooth tension tests without indications of EAC. These cases have usually been related to environments which can produce localized corrosion or hydrogen charging of the test specimen, which produces a decrease in specimen ductility without producing brittle cracking. For these cases in particular, visual and scanning electron microscopic examination of the fracture surface and gauge section areas is recommended.

SSR Ratio Considerations

The SSR ratios for the A289 test program, which includes four sets of comparative results (i.e., Test 1A-A versus Test 1B, Test 1A-B versus Test 1B, Test 2A versus Test 2B, and Test 2C versus Test 2B) are summarized in Table 2. The following SSRT parameters were employed in assessing the material susceptibility to the environmentally assisted cracking and are summarized in

Ultimate Tensile Strength Ratio (*RSU*):

1. Elongation at Fracture Ratio (*REF)*
2. Total Elongation Ratio (*RTE*):

3. Reduction in Area Ratio (*RRA*):
4. Time-to-Failure Ratio (*RTTF*):
5. Plastic Elongation Ratio (*RE*):
6. Fracture Energy Ratio (*RFE*):

In general, SSR ratios were less than [ ]^{a,c} for all comparisons. The SSR ratios measured in the slower strain rate sensitivity tests were also consistently lower than those measured in the higher strain rate preliminary tests. This behavior is typically expected when comparing aqueous environmental test results with those of dry inert environment test results.

More significant is the fact that majority of the SSR ratio values are consistently higher than [ ]^{a,c} which suggests low susceptibility to EAC. In fact a systematic study of ranking on the basis of SSR ratio values by McIntyre et.al., (Ref.4) suggested a susceptibility ranking in the range of "immune to mildly Susceptible" for the A289 steel under the primary water environment.

Fracture Morphologies

Detailed Scanning Electron Microscopy (SEM) was conducted on all the specimens to establish the fracture morphologies. SEM surface morphologies of the gauge section and necking region were also examined to identify any SCC (pitting and crack initiation) particularly near the fracture strain regions. The complete results for all the six specimens are available in Reference 7. Typical results are illustrated in **Figures 9 through 21** in this report. **Figure 9** illustrates the classical 'cup and cone' ductile fracture typically seen in most of the test specimens. It should also be noted that there is no specific quantitative acceptance criteria for evaluating EAC susceptibility of the tested material provided in ASTM Method G129 based on the SSR ratios. The only guidance is that lower SSR ratios generally indicate increasing susceptibility to EAC.

Two distinct fracture morphologies were typically visible on the fracture surface of the specimens: Firstly a [ ]^{a,c} fracture morphology seen on all the environmental test specimens constituting in excess 90% of the fracture face. Typical fracture morphologies are illustrated in **Figures 11 to 13** and in **Figures 16 to 18**. The second type of fracture morphology occasionally seen is [ ]^{a,c} fracture initiated at [ ]^{a,c} surface close to the fracture. This type of morphology is illustrated in **Figures 19 to 21**. This type of behavior is seen at very few locations restricted to [ ]^{a,c}. It is believed that this EAC influenced regions contributed to the loss of ductility in the environmental (phase 2) tests. The quantity and depth of these circumferential micro-cracks (as observed on both the fracture surface and the gauge section surface) are typically correlated with reduction in specimen ductility (e.g., [ ]^{a,c}).

EAC SUSCEPTIBILITY CONSIDERATIONS AND CONCLUSIONS

The Slow Strain-Rate technique provides a rapid and reliable method to determine stress corrosion cracking (SCC) susceptibility of metals and alloys for a broad range of applications. The technique provides a convenient means of ranking the behavior of a range of candidate materials in a given service environment.

Although the ASTM G129 method does not provide any specific quantitative acceptance criteria for evaluating EAC susceptibility, reasonable guidance and acceptability considerations can be argued from the totality of test data obtained from the A289 alloy test program.

The stress–strain test data and the SSR ratio data discussed above suggests reasonable assurance that the material, although exhibited obviously expected slight sensitivity to aqueous environment compared to the dry tests, is predominantly sound and exhibited toughness and ductile plasticity under tensile loading in the primary water environment. The reduction in SSR ratios when assessed with criteria suggested in the literature (Ref. 4) shows that its performance can be ranked between "immune" to "mildly susceptible" category.

Overall, the 18Cr-18Mn material SSR tests displayed sufficiently adequate resistance to SCC in primary water and therefore is acceptable for the intended retaining ring application. The following inferences can be considered relevant from the test results:

- The tests were successfully completed at the two strain rates, which employed duplicate test samples at each strain rate.
- The failure mode was primarily [ ]^{a,c}.
- Although there was a noticeable loss in the percentage elongation [ ]^{a,c} in the wet RCS environment in comparison with the inert environment dry test results, the detailed SEM examinations [ ]^{a,c} revealed that this can be attributed to the [ ]^{a,c}. These locations are also often found to be associated with heavy machining scars or inclusion sites on the surface. The plastic strain levels are expected to be above 20% at these locations.
- Recent industry data shows that SCC initiation at such high strain levels is a normally expected phenomenon in aqueous environments even in austenitic stainless steels. Recent industry data show that SCC can be expected even in 300 series stainless steels and Alloy 690 at the strain levels exceeding 18%-20% (Ref. 9, 10, 11).

Based on the above arguments, there is strong evidence to support the adequacy of the 18-18 stainless steel for the RCP retainer ring service requirements.

In addition to the above the probability of exposure to primary fluid for the retainer ring is significantly low, exposure requires an unlikely breach in the Alloy 625 can material. Alloy 625 has been shown through successful industry experience to be resistant to cracking in primary water environments.

Table 1. Overall SSR Test Matrix

	Screening Tests (Phase 1)			Susceptibility Tests (Phase 2)		
	Test 1A-A	Test 1A-B	Test 1B	Test 2A	Test 2C	Test 2B
Strain Rate (1/s)	[ ]a,c	[ ]a,c	[ ]a,c	[ ]a,c	[ ]a,c	[ ]a,c
Test Environment	[ ]a,c	[ ]a,c	[ ]a,c	[ ]a,c	[ ]a,c	[ ]a,c
Temperature (°F)	[ ]a,c	[ ]a,c	[ ]a,c	[ ]a,c	[ ]a,c	[ ]a,c
Pressure (psig)	[ ]a,c	[ ]a,c	[ ]a,c	[ ]a,c	[ ]a,c	[ ]a,c

Table 2. SSR Test Result Summary

	Screening Tests (Phase 1)					Susceptibility Tests (Phase 2)				
	Water	Water	Control	**Ratio$_{1A-A}$**	**Ratio$_{1A-B}$**	Water	Water	Control	**Ratio$_{2A}$**	**Ratio$_{2C}$**
	Test 1A-A	Test 1A-B	Test 1B			Test 2A	Test 2C	Test 2B		
Elastic Modulus (ksi)	[				] a,c	[				] a,c
0.02% Yield Strength (ksi)										
0.2% Yield Strength (ksi)										
Ultimate Tensile Strength (ksi)										
Elongation at Fracture (EF, %)[1]										
Elongation at Fracture (EF, inches)[1]										
Total Elongation (TE, %)[2]										
Total Elongation (TE, inches)[2]										
Area Reduction (RA, %)[2]										
Time-to-Failure (TTF, hrs)										
Plastic Elongation ($E_{0.02\%}$, inches)										
Plastic Elongation ($E_{0.2\%}$, inches)										
Fracture Energy (FE, ksi)										

[1] Based on pressure- and compliance-compensated servo positional measurements.

[2] Based on image analysis of fractured specimen.

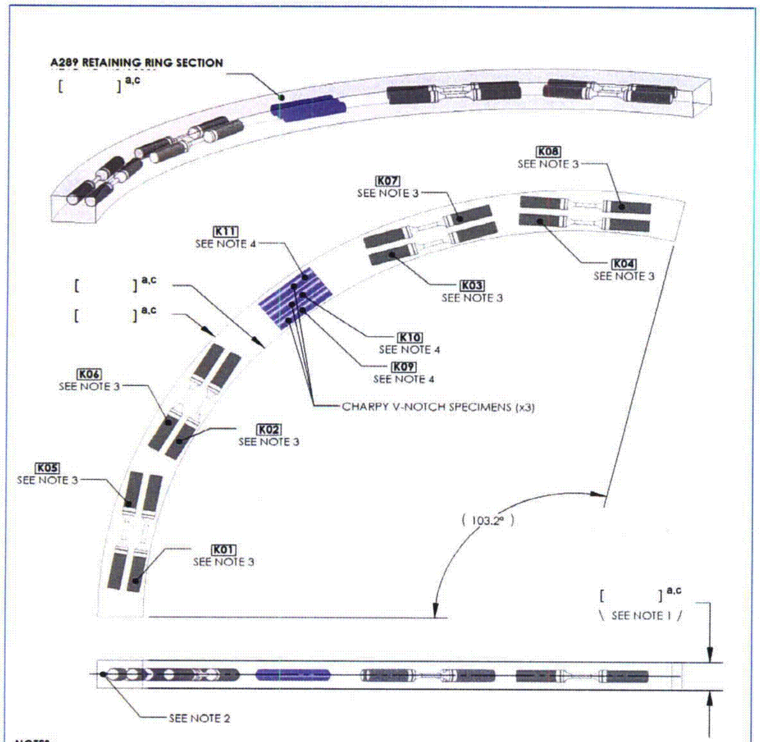

NOTES:

1. IT IS UNDERSTOOD THAT ACTUAL THICKNESS OF RING SECTION IS SLIGHTLY UNEVEN. A MINIMUM THICKNESS OF 1.0" CAN BE ASSUMED.
2. SPECIMENS SHALL BE ACQUIRED FROM THE SAME CUT PLANE IN THE RING (E.G., ALL SPECIMENS CUT WITH THE CENTRAL AXIS AT THE MID-HEIGHT OF THE RING).
3. SSRT SPECIMENS SHALL BE UNIQUELY IDENTIFIED AS SHOWN AND SHALL BE TRACEABLE THROUGHOUT MACHINING PROCESS SUCH THAT IDENTIFICATION CAN BE MADE OF THE LOCATION IN THE RING FROM WHICH THE SPECIMEN WAS ACQUIRED. IDENTIFICATION SHALL BE MADE THROUGH STAMPING OR ETCHING OF THE NON-GAUGE/SHOULDER SECTION OR BY KEEPING THE SPECIMENS IN MARKED BAGS. BOTH ENDS OF THE SSRT SPECIMENS SHALL HAVE MARKINGS TO ALLOW FOR CONTINUED IDENTIFICATION AFTER FRACTURE.
4. MACHINED CHARPY SPECIMEN DIMENSIONS SHALL MEET REQUIREMENTS OF ASTM E23-07, TYPE A SIZE. NOTCHES SHALL BE ORIENTED TOWARD THE INSIDE DIAMETER (ID) OF THE RING SECTION. SHARPY SPECIMENS SHALL BE UNIQUELY IDENTIFIED AS SHOWN.

Figure 3. SSR Test Specimen Layout in the Test Coupon

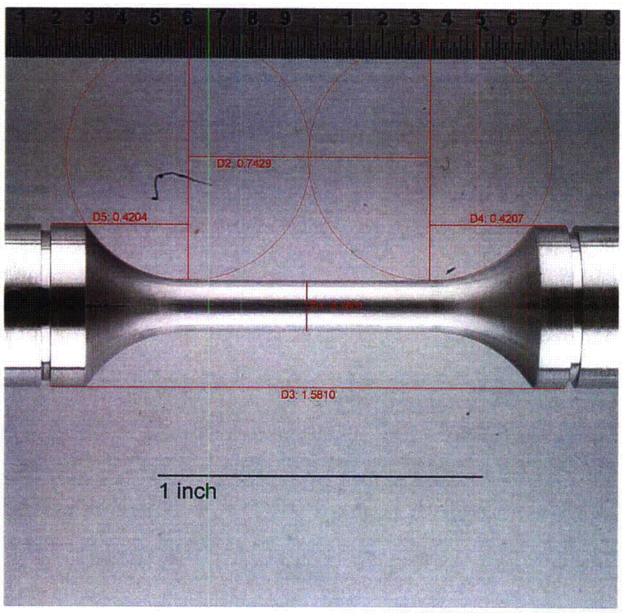

Figure 4. Typical Geometry of the Test Specimen

[ ]a,c

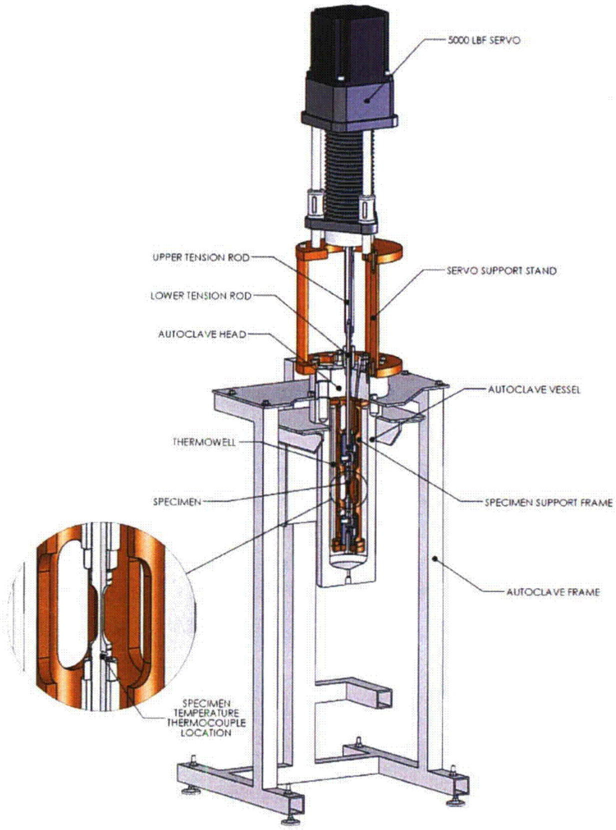

Figure 5. SSR Test Rig Design Overview

a,c

Figure 6. Overall SSR Test Program Stress-Strain Data Comparison

a,c

Figure 7. SSR Test Program Stress-Strain Data Comparison
(Preliminary Screening Tests, Phase 1)

a,c

Figure 8. SSR Test Program Stress-Strain Data Comparison
(Lower Strain Rate Susceptibility Tests, Phase 2)

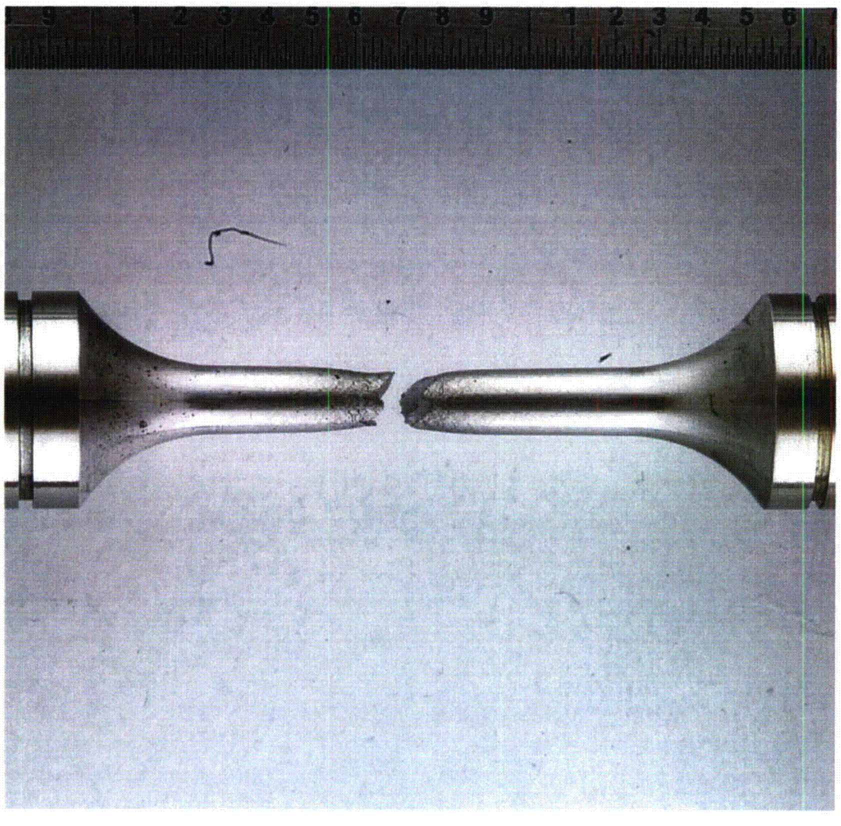

Figure 9. Typical Cup and Cone Ductile Fracture Seen in all the Specimens

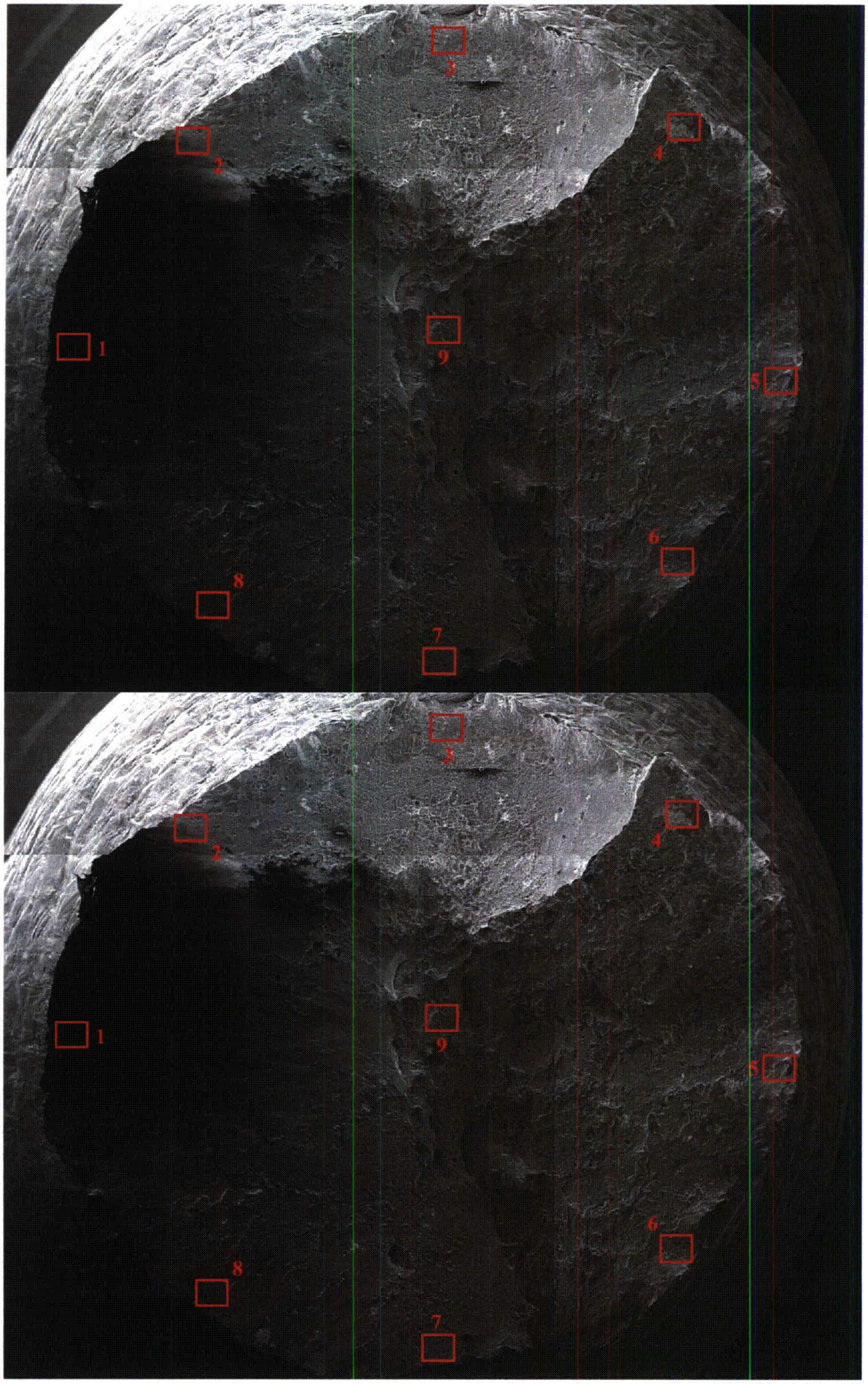

Figure 10. [ ]^{a,c} **– SEM Fracture Surface Composite (Annotated)**

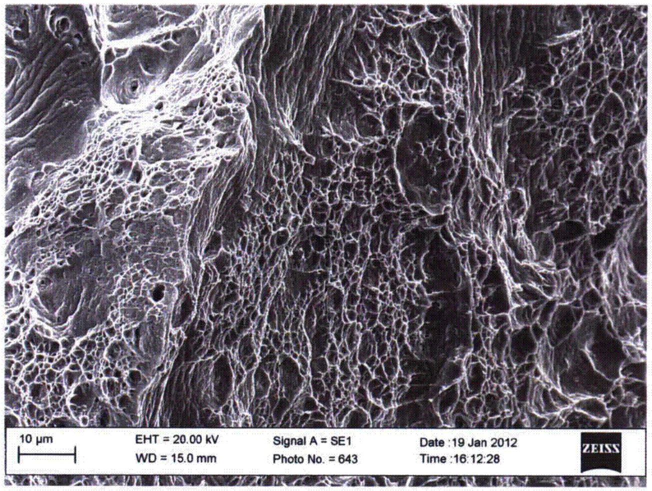

Figure 11. [ ][a,c] – SEM Fracture Surface Spot 9, Illustrating [ ][a,c] Morphology

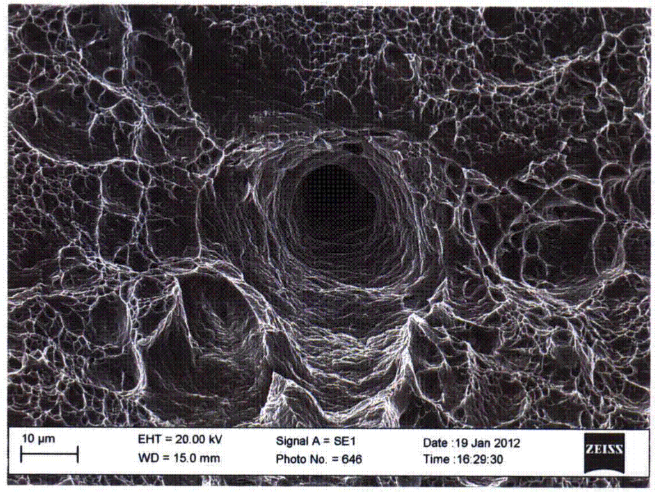

Figure 12. [ ][a,c] – SEM Fracture Surface Spot 12, Illustrating [ ][a,c] Morphology

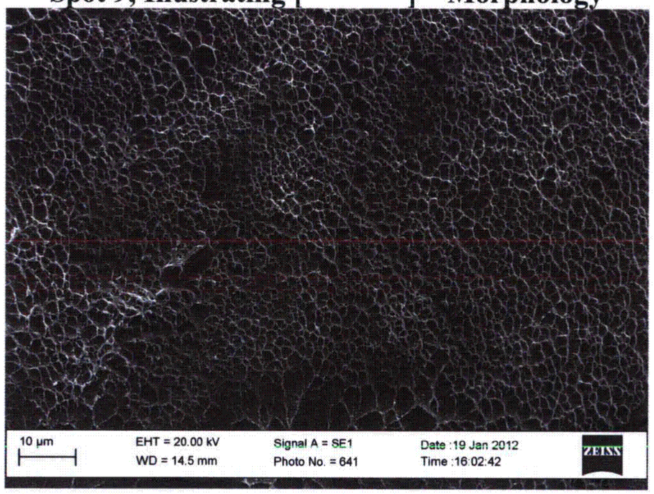

Figure 13. [ ][a,c] – SEM Fracture Surface Spot 7, Illustrating [ ][a,c] Morphology

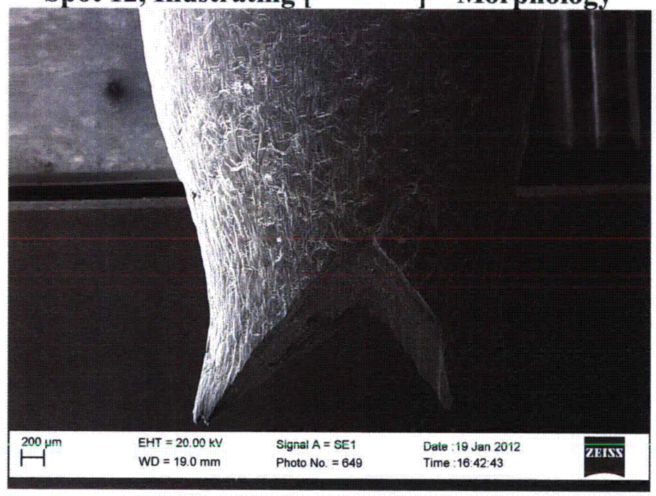

Figure 14. [ ][a,c] – SEM Gauge Section

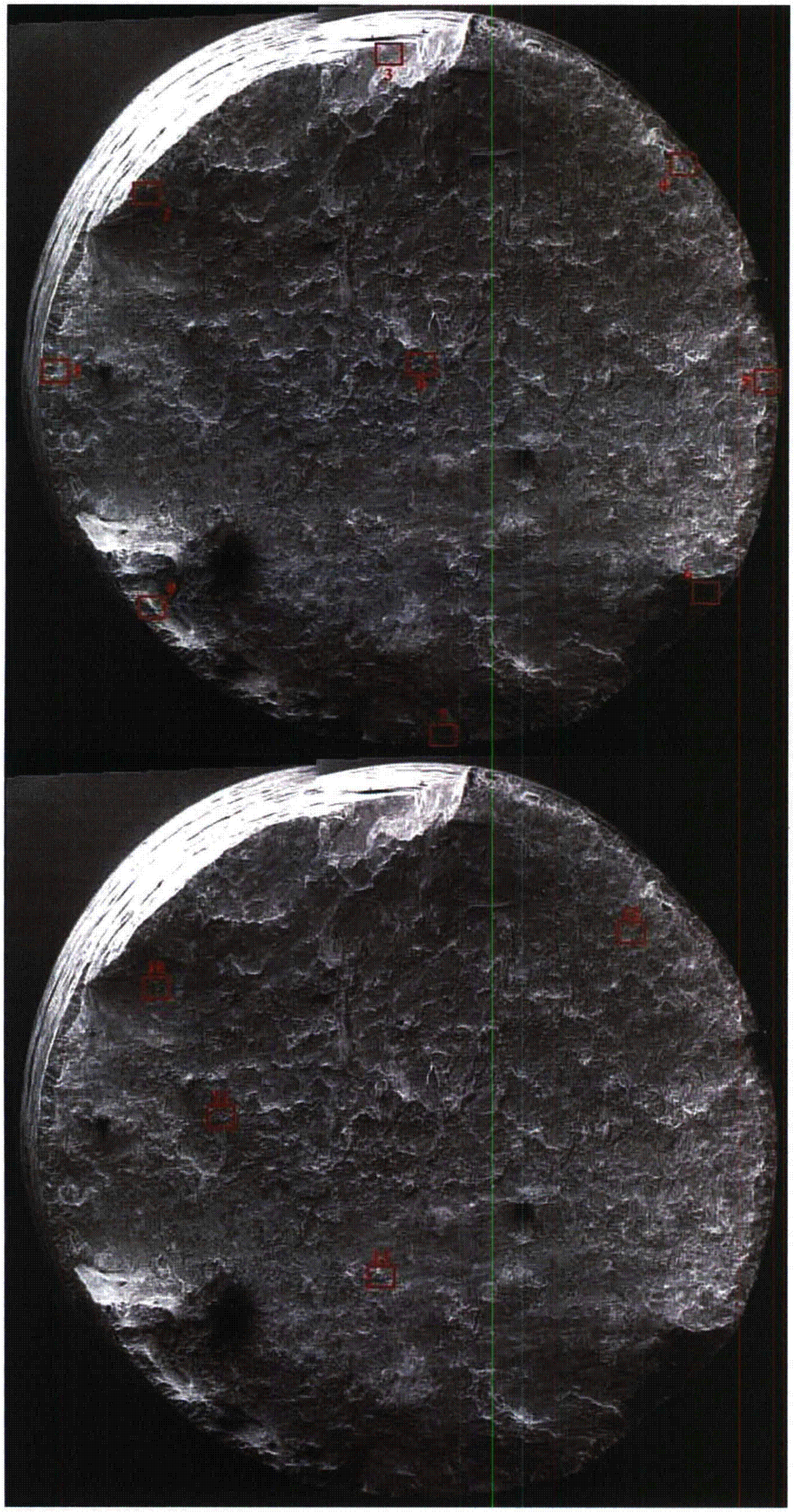

Figure 15. [ ][a,c] **– SEM Fracture Surface Composite (Annotated)**

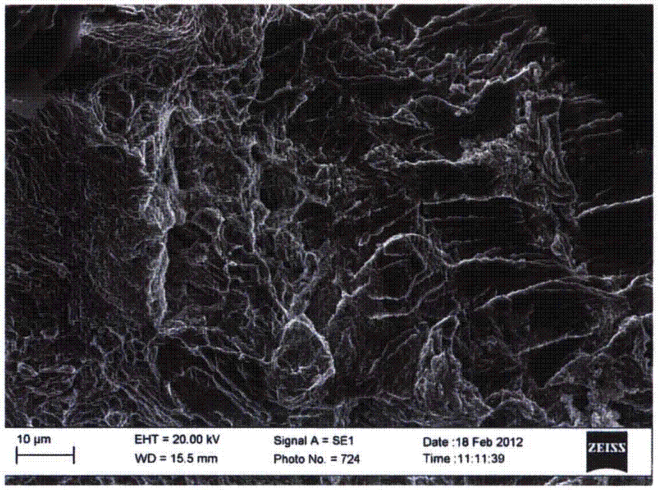

Figure 16. [ ]^{a,c} – SEM Fracture Surface Spot 4, Illustrating [ ]^{a,c}

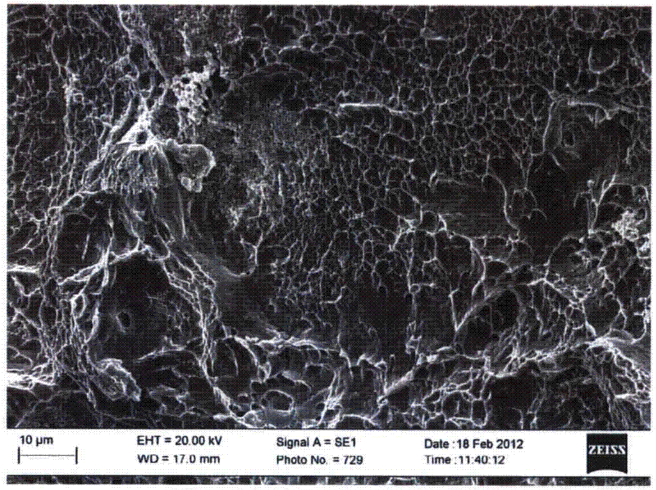

Figure 17. [ ]^{a,c}) – SEM Fracture Surface Spot 9, Illustrating [ ]^{a,c}

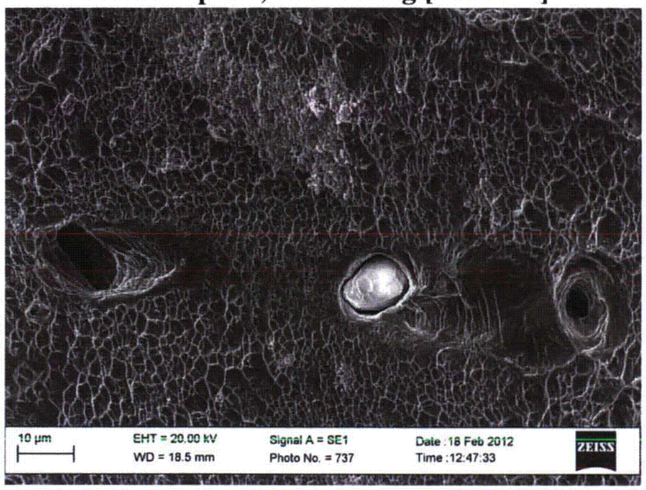

Figure 18. [ ]^{a,c} – SEM Fracture Surface Spot 10, Illustrating [ ]^{a,c}

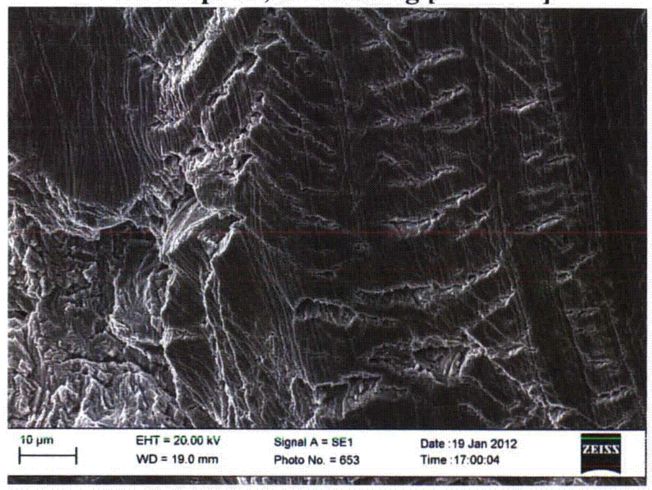

Figure 19. [ ]^{a,c} – SEM Gauge Section Necked Region Photo 4, Illustrating [ ]^{a,c}

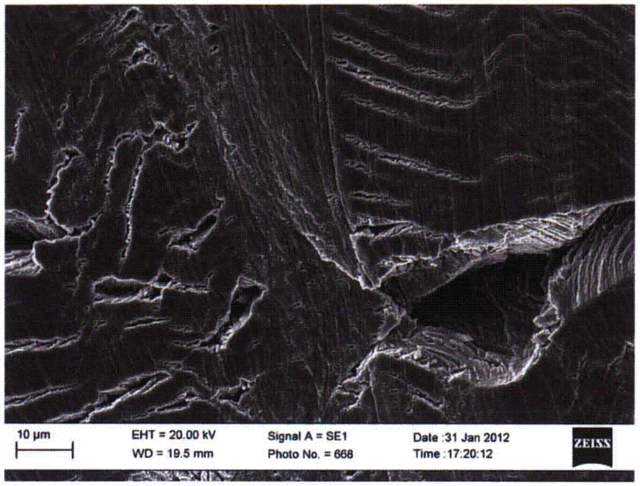

Figure 20. [ ]^{a,c} – SEM Gauge Section Necked Region Photo 4, Illustrating [ ]^{a,c}

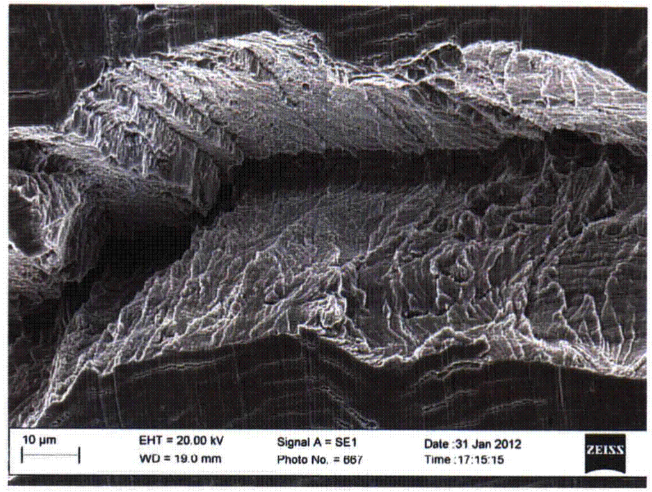

Figure 21. [ ]^{a,c} – SEM Gauge Section Necked Region Photo 3, Illustrating [ ]^{a,c}

REFERENCES

1. P. McIntyre et al, "A Comparison of the Properties of Krups 18Mn 18Cr End Rings with those of 18Mn 4Cr End Rings," Second International Colloquium P900 Retaining Ring Material, September 1985; Edited by G. Stein, W. Rensing.

2. Advanced Material for Generator Retaining Rings: Dr. Juergen Ewald, Raymond Baumgartner.

3. EPRI EL-5825 Project 2719-1 Proceedings, "Proceedings: Generator Retaining-Ring Workshop," May 1988.

4. D. R. McIntyre et al, "Slow Strain Rate Testing for Materials Evaluation in High Pressure H_2S Environments," Corrosion, Vol. 44, No. 12, Dec.1988.

5. J. H. Payer et al, "Evaluation of Slow Strain-Rate Stress Corrosion Tests Results," ASTM STP 665 1979, pp 61-77.

6. ASTM G129-00, "Standard Practice for Slow Strain Rate Testing to Evaluate the Susceptibility of Metallic Materials to Environmentally Assisted Cracking," 2000.

7. [ ]a,c

8. ASTM E8-06, "Standard Test Methods for Tension Testing of Metallic Materials," 2000.

9. O. Raquet et al, "SCC of Cold-Worked Austenitic Stainless Steels in PWR Conditions", Advances in Materials Science, Vol. 7, No. 1 (11), March 2007.

10. "Stress Corrosion Crack Growth Behavior of Cold-Worked 304L and 316L Stainless Steels", EPRI, Palo Alto, CA: 2002. 1007379.

11. "Resistance of Alloys 690, 152 and 52 to PWSCC", Presented at Alloy 690 Meeting, NRC RES, May 2008.

REVISION HISTORY

REV	DATE	REVISION DESCRIPTION
0	n/a	Not used
1	November 2012	Initial revision issued as the Non-Proprietary Class 3 version of APP-MP01-T2-002, Revision 1